

## A COMPTON-SUPPRESSION SPECTROMETER FOR $\gamma$ - $\gamma$ COINCIDENCE MEASUREMENTS: LARGE SOLID ANGLE AND EXCELLENT SUPPRESSION

H.J.M. AARTS, C.J. VAN DER POEL, D.E.C. SCHERPENZEEL, H.F.R. ARCISZEWSKI and G.A.P. ENGELBERTINK

*Fysisch Laboratorium, Rijksuniversiteit Utrecht, PO Box 80.000, Utrecht, The Netherlands*

Received 2 June 1980

For  $\gamma$ - $\gamma$  coincidence measurements a Compton-suppression spectrometer with a large solid angle of 120 msr and excellent suppression has been designed. The dimensions of the NaI anticoincidence shield have been optimized by means of Monte Carlo calculations. The NaI shield has a length of 35 cm and a diameter of 30 cm. A 20% efficient HPGe crystal with a dead layer of 0.22 mm and a hollow core is used as central detector. For  $^{60}\text{Co}$ , the average suppression of the Compton background between 100 and 1100 keV amounts to 11.8 with a photopeak loss of 5.8%. The areas of the 1173 and 1332 keV peaks taken together amount to 60% of the total number of registered counts for the suppressed spectrum and to 15% for the non-suppressed spectrum. The spectrometer has been tested in a  $\gamma$ - $\gamma$  coincidence experiment with the reaction  $^{24}\text{Mg} + (45 \text{ MeV})^{16}\text{O}$ .

### 1. Introduction

In  $\gamma$ -ray spectroscopy with reactions induced by  $\alpha$ -particles or heavy ions, the complexity of the spectra and the low yield of many transitions of interest, call for spectrometers with high resolution, low background and large efficiency. The background due to Compton scattering can be removed to a great

extent by surrounding the detector by an anticoincidence shield.

Two different configurations of the shield have been reported [1-5]. The symmetrical Compton-suppression spectrometer [4] consists of a coaxial shield with a hollow core of the central detector. The incoming  $\gamma$ -ray beam is oriented along the cylinder axis. The advantage of this geometry is the variable

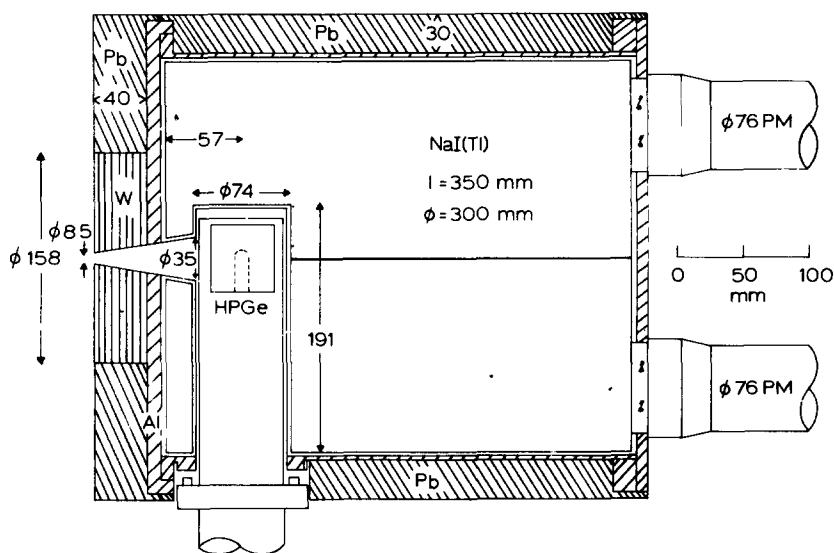


Fig. 1. Schematic drawing of the Compton suppression spectrometer with a solid angle of 120 msr. The distance from the source to the central detector is 100 mm. The dimensions are given in mm.

solid angle of the system which leads to a variable average Compton suppression. It is, however, difficult to eliminate events which correspond to small-angle scattering and which leave little energy in the central detector. The geometry is especially disadvantageous for high-energy  $\gamma$ -rays, since Compton scattering is then peaked in the forward direction. The symmetrical set-up therefore leads to low Compton suppression in the low-energy part of the spectrum. In addition double-escape peaks are not suppressed very well, due to the presence of collinear holes in the shield.

The above mentioned disadvantages are circumvented in the asymmetrical configuration shown in fig. 1, where the central detector is oriented at a right-angle to the direction of the incoming radiation.

Optimization of the Compton suppression of such an apparatus with disregard of the solid angle leads automatically to a small photon entrance hole and to a relatively large distance between an external source and the central detector with, as a consequence, a rather small solid angle. Examples are the spectrometers of refs. [2] and [3] with solid angles of 7 and about 4 msr, respectively. These spectrometers are very suitable for singles measurements, such as those of a singles spectrum or of an angular distribution, where a large  $\gamma$ -ray flux compensates the small solid angle.

In  $\gamma$ - $\gamma$  coincidence experiments, however, in which a CSS is combined typically with three or four gating Ge(Li) detectors of about 400 msr solid angle each, the combination is very poorly matched.

The present paper describes an asymmetrical CSS with a solid angle of 120 msr and an excellent Compton suppression. The dimensions of the NaI anticoincidence shield are optimized by means of Monte Carlo calculations, which are described in ref. [5].

## 2. Design

The large solid angle of the spectrometer is obtained by making the minimum distance between the external source and the central crystal relatively short and the diameter of the  $\gamma$ -ray entrance hole large. The short minimum distance of course restricts the thickness of the NaI and the amount of passive shielding at the front side. In the present set-up the diameter of the entrance hole is limited by the dimensions of the central detector.

With a large solid angle chosen in this way, Monte

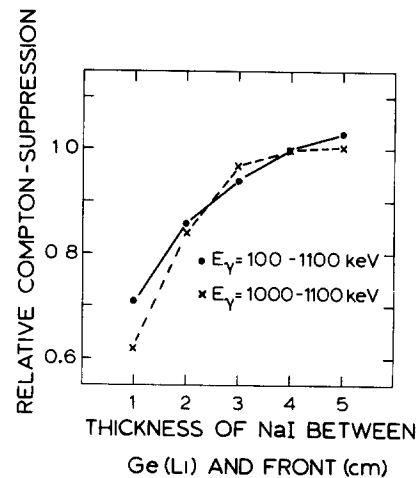


Fig. 2. The Monte Carlo result for the relative Compton suppression as a function of the thickness of NaI at the front side for  $^{60}\text{Co}$ . The energy regions 100–1100 keV and 1000–1100 keV of the  $^{60}\text{Co}$  spectrum of the central detector are considered. Both curves are arbitrarily normalized to unity for a thickness of 4 cm.

Carlo calculations are performed to investigate the other dimensions of the asymmetrical CSS to obtain as good a Compton suppression as possible. The CSS configuration considered is shown in fig. 1. The performance of this configuration has been studied as a function of the following parameters: the thickness of the NaI anticoincidence shield at the front side,

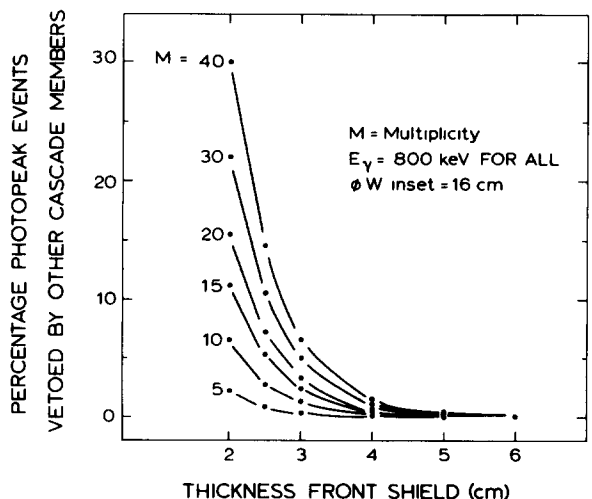


Fig. 3. The Monte Carlo result for cascade suppression as a function of the thickness of the passive front shield. The calculation has been performed for a cascade with multiplicity  $M = 5, 10, 15, 20, 30$  and  $40$  of which all members have an energy of 800 keV. The present front shield (see fig. 1) has a thickness of 4 cm.

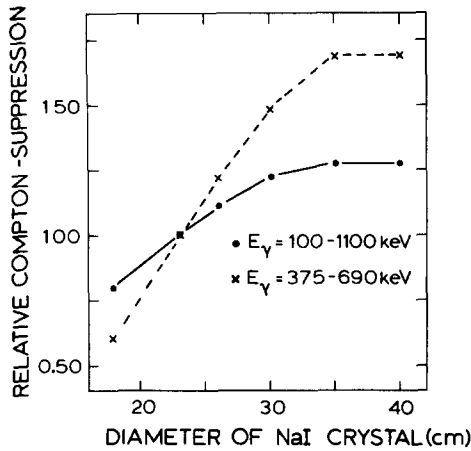


Fig. 4. The Monte Carlo result for the relative Compton suppression as a function of the diameter of the NaI shield for  $^{60}\text{Co}$ . The energy regions 375–690 keV and 100–1100 keV of the  $^{60}\text{Co}$  spectrum of the central detector are considered. Both curves are arbitrarily normalized to unity for a diameter of 23 cm.

the amount of passive shielding, the diameter of the  $\gamma$ -ray entrance hole, the length and the diameter of the surrounding NaI anticoincidence shield.

The Monte Carlo calculations are similar to those reported in ref. [5]. The results are presented in figs. 2–5 which show the relative Compton suppression as a function of the parameter considered. It should be remarked that the results are obtained with the other parameters kept fixed at the values given in fig. 1.

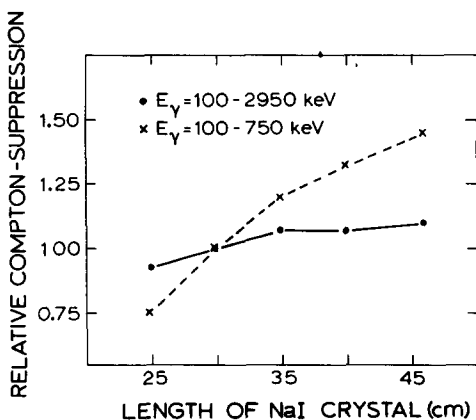


Fig. 5. The Monte Carlo result for the relative Compton suppression as a function of the length of the NaI shield for a 3 MeV  $\gamma$ -ray. The energy regions 100–750 keV and 100–2950 keV of the spectrum of the central detector are considered. Both curves are arbitrarily normalized to unity for a length of 30 cm.

### 2.1. The thickness of the NaI shield at the front side

The main function of the NaI shield between the central detector and the front of the spectrometer is to detect photons which are scattered over a large angle. Reduction of this part of the shield will therefore result in more Compton background close to the Compton edge. Fig. 2 gives the Monte Carlo result for the relative Compton suppression as a function of the thickness of NaI at the front side for  $^{60}\text{Co}$ . The energy regions 100–1100 keV and 1000–1100 keV of the  $^{60}\text{Co}$  spectrum of the central detector are considered. Both curves are relative and arbitrarily normalized to unity for a thickness of 4 cm. In view of the short minimum distance desired, a thickness of 2 cm NaI is chosen.

### 2.2. The shielding lead front plate

Reduction of the thickness of the lead front plate increases the probability for an unwanted photon to reach the anticoincidence shield and to produce a veto signal. A  $\gamma$ -ray cascade of high multiplicity has to be considered in this respect. When a member of a cascade of multipolarity  $M$  strikes the central detector then, angular correlation effects neglected, about  $(M-1)/2$   $\gamma$ -rays will *simultaneously* hit the shielding front plate. Insufficient shielding at the front will thus cause suppression of  $\gamma$ -ray cascades with high multiplicity. The effective shielding of the front plate is increased by replacing the important central part of the lead by a 16 cm diameter inset of densimet, a W-Fe alloy (1.2% Fe) with a density of 18 g/cm<sup>3</sup> (see fig. 1).

The Monte Carlo result for cascade suppression as a function of the thickness of the front plate is shown in fig. 3. The calculations have been performed for a cascade with multiplicity  $M = 5, 10, 15, 20, 30$  and 40 of which all members have an energy of 800 keV. Fig. 3 shows that for the chosen thickness of 4 cm the cascade suppression is less than 2%, even for high multiplicities.

### 2.3. The diameter of the $\gamma$ -ray entrance hole

Gamma-rays, which are scattered back from the central detector to the entrance hole, give rise to the inevitable Compton edge. A large-diameter entrance hole, a prerequisite for a large solid angle, leads necessarily to a relatively high Compton edge. Its position,

however, is at a known energy distance from the corresponding photopeak.

In the present set-up the diameter of the entrance hole is chosen as large as allowed by the 50 mm diameter of a 20% efficient Ge detector. The entire central crystal is practically irradiated.

#### 2.4. The diameter and the length of the NaI anticoincidence shield

Figure 4 shows (again for  $^{60}\text{Co}$ ) the Monte Carlo result for the relative Compton suppression as a function of the diameter of the NaI shield. Apart from the overall suppression in the energy region 100–1100 keV, the region from 375–690 keV is also considered. In the latter the suppression is predominantly determined by the diameter of the shield as is shown in fig. 4. A diameter of 30 cm has been chosen.

The length of the anticoincidence shield mainly affects the suppression of photons which in the central crystal are scattered over a small angle. Since  $\gamma$ -rays of higher energy scatter more in the forward direction, a  $\gamma$ -ray of 3 MeV is used to investigate the Compton suppression as a function of the length of the NaI crystal. Fig. 5 shows the result for the relative Compton suppression for the energy regions 100–

750 keV and 100–2950 keV. Both curves are arbitrarily normalized to unity for a length of 30 cm. A length of 35 cm was chosen.

#### 2.5. The final configuration and electronics

The geometry and dimensions of the NaI anticoincidence shield, discussed above, are shown in fig. 1. The conical entrance hole corresponds to a position of the source at 16 mm in front of the spectrometer i.e. the usual target position. The distance from the source to the central detector is now 10.0 cm. The solid angle of the spectrometer amounts to 120 msr or 0.96% of  $4\pi$ . The half-angle subtended is  $11^\circ$ .

The NaI shield is divided into four optically separated sections, to allow a high count rate (up to  $6 \times 10^5 \text{ s}^{-1}$ ) in the shield without overloading the photomultiplier tubes. This division also makes it possible to use the system as a pair-spectrometer.

The anode signal of each of the four PM tubes is fed into a constant fraction discriminator (CFD, Canberra 1326 D) via a timing filter amplifier (TFA, ORTEC 454). The output pulses of the four CFDs are collected in a mixer which then produces the final veto signal (see fig. 6).

A modified CFD which generates the timing signal

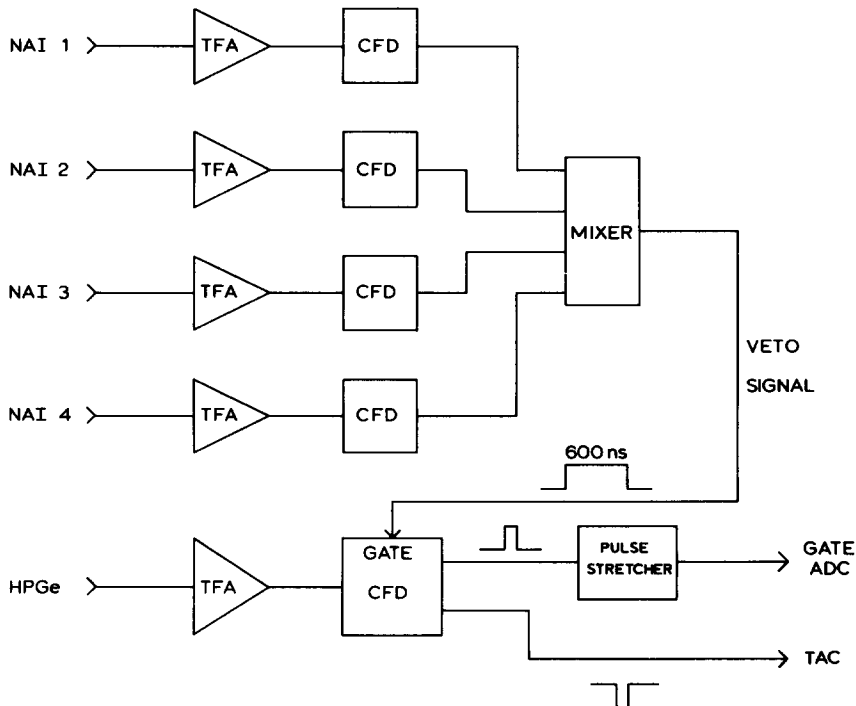


Fig. 6. Block diagram of the electronics used, see section 2.5

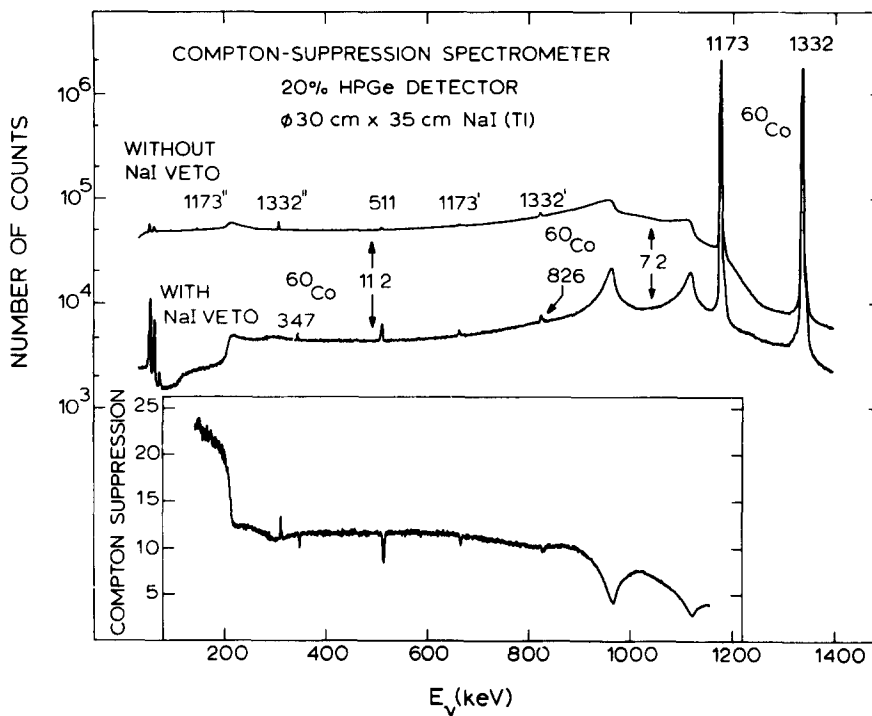


Fig. 7 Spectrum of  $^{60}\text{Co}$ , with and without Compton suppression. The inset gives the ratio between the channel contents of the upper and the lower spectrum, i.e. the Compton suppression as a function of the energy. The average Compton suppression between 100–1100 keV amounts to 11.8. The weak 347 and 826 keV peaks belong to the  $^{60}\text{Co}$  decay (see text). The relatively large Compton edges in the suppressed spectrum reflect the large solid angle.

of the central Ge detector is gated by the veto pulse, so that only non-vetoed timing signals are selected.

For a singles spectrum this selected timing signal is, after stretching, supplied to the gate input of an analog-to-digital converter (ADC) for prompt coincidence with the energy signal of the central detector.

In a coincidence experiment this selected timing signal is fed into the start of a time-to-amplitude converter (TAC).

### 3. Performance of the spectrometer

The pulse-height resolution of the four sections of the NaI shield \* varies between 11.8–12.9% for the 662 keV  $\gamma$ -ray from  $^{137}\text{Cs}$ . The lowest detectable energy above the noise is 28 keV. Coincidences between two sections give a time peak with a fwhm of 5.5 ns.

A HPGGe crystal \* with a thin dead layer of 215  $\mu\text{m}$

\* Manufactured by Harshaw Chemie B V, De Meern, The Netherlands.

is used as a central detector. Such a crystal improves the Compton suppression in the region of the Compton edge, as escape photons of low energy can easily reach the surrounding shield to produce a veto signal, see ref. [5]. The width of 600 ns for the veto signal is based on the time jitter of the HPGGe signal and is chosen to guarantee a good overlap between the veto signal and the HPGGe time pulse. This width therefore depends on the timing quality of the central detector.

#### 3.1. Results for $^{60}\text{Co}$ and $^{56}\text{Co}$

To test the spectrometer spectra of  $^{60}\text{Co}$  have been recorded with a 61  $\mu\text{Ci}$  source at the target position, 16 mm before the front plate (see fig. 1). Fig. 7 shows the spectra with and without Compton suppression. The spectra were accumulated for 1.5 h. The non-suppressed count rate in the central detector was 24 000  $\text{s}^{-1}$ , the suppressed count rate 6000  $\text{s}^{-1}$ . The large solid angle is reflected in the relatively large Compton edges in the suppressed spectrum. See for comparison fig. 5 of ref. [5] where the solid angle is a factor of 16 smaller.

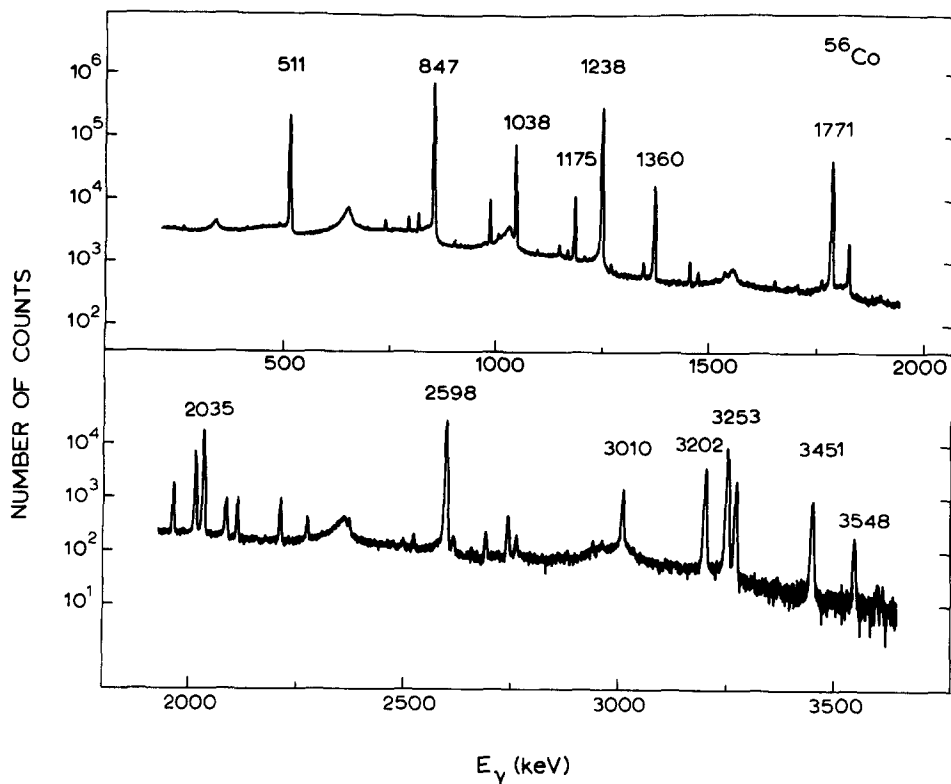


Fig. 8. Compton-suppressed spectrum of  $^{56}\text{Co}$ .

Figure 7 also gives the Compton suppression as a function of energy. The average Compton suppression between 100–1100 keV amounts to 11.8. The loss of pulses in the photopeaks amounts to 5.8%.

The areas of the 1173 and 1332 keV peaks taken together amount to 60% of the total number of

Table 1

Characteristic quantities of the Compton-suppression spectrometer with 120 msr solid angle

Anti-coincidence shield	
Material	NaI
Dimensions	See fig 1
Lowest detectable energy	28 keV
Central detector	
Type	HPGe
Dead layer thickness	215 $\mu\text{m}$
Volume	90 $\text{cm}^3$
Results for $^{60}\text{Co}$	
Compton suppression for 100–1100 keV	11.8
Photopeak loss	5.8%
Peak-to-total ratio	60%

registered counts for the suppressed spectrum and 15% for the non-suppressed spectrum.

The excellent Compton suppression is demonstrated by the appearance of the 347 and 826 keV peaks, which belong to the  $^{60}\text{Co}$  decay. The 347 keV  $\gamma$ -ray originates from the same level as the 1173 keV  $\gamma$ -ray, but with  $I_{347}/I_{1173} = 7.6 \times 10^{-5}$ , see ref. [6]. The 826 keV  $\gamma$ -ray, a little higher in energy than the single-escape peak of 1332 keV, is the main branch from the  $^{60}\text{Ni}$  level at 2159 keV, which is fed by the 347 keV transition.

Some characteristic quantities of the spectrometer are given in table 1.

Figure 8 shows the more complex spectrum of  $^{56}\text{Co}$ . The Compton edges associated with the strongest photopeaks are rather pronounced. This is the price to be paid for the large solid angle.

### 3.2. In-beam $\gamma$ - $\gamma$ coincidence results

The spectrometer described here was designed for studies of discrete high-spin fast states of sd- and f-shell nuclei. In these investigations,  $\gamma$ - $\gamma$  coincidence

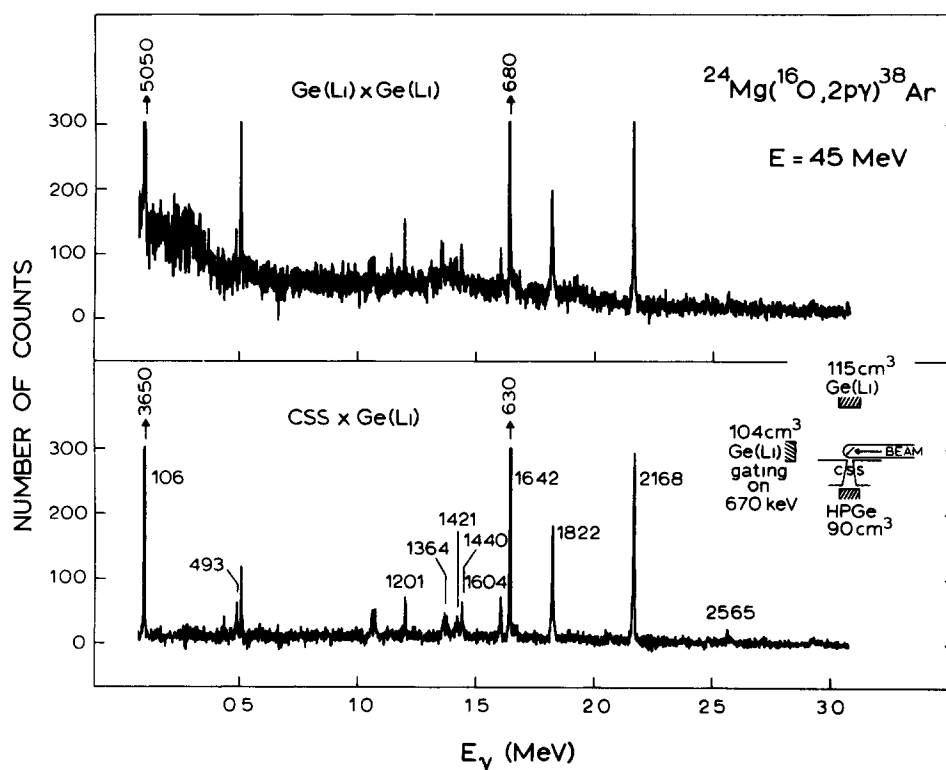


Fig 9. Spectra from the  $^{24}\text{Mg}(^{16}\text{O}, 2p)^{38}\text{Ar}$  reaction, coincident with the 670 keV  $\gamma$ -ray observed at  $0^\circ$  in the geometry as shown in the insert. The upper coincidence spectrum is recorded with a bare  $115\text{ cm}^3$  Ge(Li) detector at a distance of 11 cm. The lower coincidence spectrum is recorded with the CSS. The spectra are corrected for background and random phenomena (see section 3.2).

measurements play a major role [7–13]. To compare the present CSS with a bare Ge(Li) detector a  $\gamma$ – $\gamma$  coincidence experiment was performed. To facilitate the comparison, the set-up shown in the insert of fig. 9 was chosen. The CSS with  $d\Omega = 120$  msr was placed at  $\theta_\gamma = +90^\circ$  and a bare Ge(Li) detector with  $d\Omega = 160$  msr (11 cm distance) at  $\theta_\gamma = -90^\circ$ . The solid angles thus are about equal. A second bare Ge(Li) which serves as gate detector for the CSS as well as for the  $115\text{ cm}^3$  Ge(Li) was situated at  $\theta_\gamma = 0^\circ$ . A  $300\text{ }\mu\text{g}/\text{cm}^2$   $^{24}\text{Mg}$  target, enriched to 99.94%, on a  $25\text{ }\mu\text{m}$  Au backing was bombarded with a 45 MeV  $^{16}\text{O}^{6+}$  beam of 100 nA (electrical). With the geometry, reaction, beam energy and target thickness given, the beam current was limited by the maximum count rate of about  $25\,000\text{ s}^{-1}$  of the three Ge detectors. The real-to-random ratio in the time spectra Ge(Li)  $\times$  Ge(Li) and CSS  $\times$  Ge(Li) was about 13.

During the experiment a wide, approximate gate was set electronically around the 670 keV peak in the gate detector at  $\theta_\gamma = 0^\circ$ . The 670 keV  $\gamma$ -ray was pro-

duced strongly in the decay of high-spin states in  $^{38}\text{Ar}$  (ref. [13]). The coincidence events, accumulated during 48 h, are recorded on magnetic tape. In the off-line analysis a proper (much narrower) gate is set on the 670 keV peak. The final spectra, shown in fig. 9, have been corrected for background and random phenomena.

The data in fig. 9 clearly show the advantage of the present large-solid-angle CSS in  $\gamma$ – $\gamma$  coincidence measurements.

#### 4. Discussion

The present spectrometer (fig. 1) combines a large solid angle of 120 msr with an excellent Compton suppression. Other spectrometers reported recently in the literature have smaller solid angles and lower Compton suppression. A comparison is made in table 2.

The large solid angle makes the apparatus very

Table 2  
Comparison of some recent Compton-suppression spectrometers

Ref	Solid angle (msr)	Average Compton suppression ( $^{60}\text{Co}$ , 100–1100 keV)
Konijn et al [1]	$\approx 75$	$\approx 8$
Van Driel et al [2]	7	10 <sup>a</sup>
Beetz et al [3]	$\approx 4$	$\approx 9$
Lindblad [4]	38	$\approx 6$
Present spectrometer	120	11.8

<sup>a</sup> See also ref [5] for use with a thin-dead-layer HPGe crystal as central detector.

suitable for  $\gamma$ – $\gamma$  coincidence measurements.

For the present spectrometer the 50 mm diameter of the central HPGe detector of 20% efficiency limits the diameter of the entrance hole of the NaI and thus the solid angle. A larger HPGe (or preferably a Gamma-X crystal, see ref. [5]) would allow an even bigger solid angle, also with good Compton suppression. A further decrease of the thickness of the NaI at the front side, another possibility in order to increase the solid angle, is not recommended as it quickly leads to a deterioration of the Compton suppression as the Monte Carlo calculation in fig. 2 shows.

The maximum count rate for the present CSS under in-beam circumstances as described in section 3.2 is limited by the count rate which the central detector can handle. This in contrast with the apparatus described in refs. [2] and [5], where the count rate of the NaI anticoincidence shield was the limiting factor.

The average Compton suppression for 100–1100 keV of  $^{60}\text{Co}$  for the present CSS was calculated by Monte Carlo techniques to be 12.9, a result reasonably close to the experimentally observed value of 11.8 in view of the approximations in the calculation [5]. A loss of 0.8% of the veto pulses in the electronic circuitry (an effect not included in the Monte Carlo calculation) would also already explain the difference.

A characteristic quantity for a spectrometer in general with respect to Compton background is the peak-to-total ratio  $P$ , i.e. the number of counts in the photopeaks divided by the total number of registered counts in the spectrum. The bare HPGe detector mentioned has for  $^{60}\text{Co}$  a peak-to-total ratio of  $P_{\text{HP}} =$

0.15. The present CSS has for  $^{60}\text{Co}$  the value  $P_{\text{CSS}} = 0.60$ . Other quantities of interest can be expressed straightforwardly in  $P_{\text{HP}}$  and  $P_{\text{CSS}}$ . For the central detector of the CSS, the ratio of non-suppressed count rate and suppressed count rate is e.g. given by  $P_{\text{CSS}}/P_{\text{HP}}$ .

In a  $\gamma$ – $\gamma$  coincidence experiment those events are of interest which correspond to a photopeak–photopeak coincidence. For two bare detectors with each  $P = 0.15$  the subset of photopeak–photopeak coincidences constitutes only 2.3% of the total number of coincidence events. For two Compton suppression spectrometers, however, each with  $P_{\text{CSS}} = 0.60$ , the photopeak–photopeak coincidences make up 36% of the total number of events. In this case the number of unwanted coincidence events written on magnetic tape is also reduced by the factor  $(P_{\text{CSS}}/P_{\text{HP}})^2 = 16$ .

The result in fig. 3 shows that the passive shielding at the front of the CSS is sufficiently thick to make cascade suppression negligible.

The performance of the spectrometer in a reaction which emits a large number of neutrons has not yet been investigated, but Lindblad [4] has successfully used a CSS in a study of the  $^{144}\text{Nd}(^{12}\text{C}, 6n\gamma)^{150}\text{Dy}$  reaction.

We like to thank D. Balke, J. Sodaar and N.A. van Zwol for their technical contributions.

This work was performed as part of the research program of the “Stichting voor Fundamenteel Onderzoek der Materie” (FOM) with financial support from the “Nederlandse Organisatie voor Zuiver Wetenschappelijk Onderzoek” (ZWO).

## References

- [1] J. Konijn, P.F.A. Goudsmit and E.W.A. Lingeman, Nucl. Instr. and Meth. 109 (1973) 83
- [2] M.A. van Driel, Thesis, R.U. Utrecht (1976).
- [3] R. Beetz, W.L. Posthumus, F.W.N. de Boer, J.L. Maarleveld, A. van der Schaaf and J. Konijn, Nucl. Instr. and Meth. 145 (1977) 353
- [4] T. Lindblad, Nucl. Instr. and Meth. 154 (1978) 53.
- [5] H.J.M. Aarts, G.A.P. Engelbertink, C.J. van der Poel, D.E.C. Scherpenzeel and H.F.R. Arciszewski, Nucl. Instr. and Meth. 172 (1980) 439.
- [6] D.C. Camp and J.R. van Hise, Phys. Rev. C14 (1976) 261.
- [7] M.A. van Driel, G.A.P. Engelbertink, H.H. Eggenhuisen, L.P. Ekstrom and J.A.J. Hermans, Phys. Lett. 59B (1975) 336



- [8] M.A. van Driel, H.H. Eggenhuisen, G.A.P. Engelbertink, L.P. Ekstrom and J.A.J. Hermans, Nucl. Phys. A272 (1976) 466.
- [9] L.P. Ekstrom, H.H. Eggenhuisen, G A P Engelbertink, J.A.J. Hermans and H.J.M. Aarts, Nucl. Phys A283 (1977) 157.
- [10] H H Eggenhuisen, L.P. Ekstrom, G.A P. Engelbertink, H.J.M. Aarts and J.A.J. Hermans, Nucl Phys A285 (1977) 167
- [11] H.H. Eggenhuisen, L.P. Ekstrom, G.A.P. Engelbertink, H.J.M. Aarts and W.G.J. Langeveld, Nucl. Phys. A299 (1978) 175.
- [12] H.H. Eggenhuisen, L.P. Ekstrom, G.A P. Engelbertink and H.J.M. Aarts, Nucl. Phys. A 305 (1978) 245.
- [13] H.J.M. Aarts, G.A.P. Engelbertink, H H. Eggenhuisen and L.P. Ekstrom, Nucl. Phys A321 (1979) 515